crystals

MDPI

Article

Study of Microstructural and Mechanical Properties of Al/SiC/TiO_2 Hybrid Nanocomposites Developed by Microwave Sintering

Manohar Reddy Mattli [1,†], Penchal Reddy Matli [2,†], Adnan Khan [1], Rokaya Hamdy Abdelatty [1], Moinuddin Yusuf [1], Abdulla Al Ashraf [1], Rama Gopal Kotalo [2] and Rana Abdul Shakoor [1,*]

[1] Center of Advanced Materials (CAM), Qatar University, Doha 2713, Qatar; manoharreddy892@gmail.com (M.R.M.); samikhanmechanical@gmail.com (A.K.); Rokaya.abdelatty@qu.edu.qa (R.H.A.); moinuddin@qu.edu.qa (M.Y.); aa.ashraf@qu.edu.qa (A.A.A.)
[2] Department of Physics, Sri Krishnadevaraya University, Anantapur 515003, India; drlpenchal@gmail.com (P.R.M.); krgverma@yahoo.com (R.G.K.)
* Correspondence: shakoor@qu.edu.qa
† Authors with equal contribution.

Abstract: Aluminum hybrid metal matrix nanocomposites (Al/SiC/TiO_2) were synthesized through a microwave-assisted powder metallurgy process, and their evolved microstructure and mechanical properties were investigated. The Al/SiC/TiO_2 hybrid nanocomposites were prepared by reinforcing aluminum (Al) matrix with a fixed amount of silicon carbide (SiC) nanoparticles (5 wt.%) and varying concentrations of titanium dioxide (TiO_2) nanoparticles (3, 6, and 9 wt.%). The morphology results revealeda uniform distribution of SiC and TiO_2 reinforcements in the aluminum matrix. An increase in the hardness and compressive strength of the Al/SiC/TiO_2 hybrid nanocomposites was noticed with the increasein TiO_2 nanoparticles. The Al/SiC/TiO_2 hybrid nanocomposites that had an optimum amount of TiO_2 nanoparticles (9 wt.%) showcased the best mechanical properties, with maximum increments of approximately 124%, 90%, and 23% of microhardness (83 $\pm$ 3 HV), respectively, yield strength (139 $\pm$ 8 MPa), and ultimate compression strength (375 $\pm$ 6 MPa) as compared to that of pure Al matrix. The Al/SiC/TiO_2 hybrid nanocomposites exhibited the shear mode of fracture during their deformation process.

Keywords: aluminum; hybrid nanocomposites; microwave sintering; hardness; compression strength

Citation: Mattli, M.R.; Matli, P.R.; Khan, A.; Abdelatty, R.H.; Yusuf, M.; Ashraf, A.A.; Kotalo, R.G.; Shakoor, R.A. Study of Microstructural and Mechanical Properties of Al/SiC/TiO_2 Hybrid Nanocomposites Developed by Microwave Sintering. *Crystals* **2021**, *11*, 1078. https://doi.org/10.3390/cryst11091078

Academic Editor: Roberto Comparelli

Received: 5 August 2021
Accepted: 2 September 2021
Published: 6 September 2021

1. Introduction

In recent years, hybrid composites have been attractive because of their multifunctional characteristics and specific properties, such as low cost, lightweight, low density, high strength to weight ratio, and ease of fabrication. Hybrid matrix composites (HMCs) are developed by the combination of two or more reinforcements incorporated into a suitable matrix to allow for a superposition of their properties. HMCs provide a combination of unique properties that cannot be realized in conventional composite materials. HMCs are highly efficient and demonstrate promising properties, and thus, their rapid utility in various applications [1,2]. The important criteria for the use of hybrid composites are based on high strength, crack propagation resistance, and plasticity exhibited at high loads. The selection of materials is of key importance in designing and producing the components that conform to the end-user requirements. The possibility of mixing different reinforcements into the hybrid composite usually leads to enhanced structural, mechanical, electrical, and thermal characteristics, making them attractive for many applications, such as automobile, aerospace, aeronautical, marine, and other engineering applications [3,4].

Aluminum hybrid matrix composites (AHMCs) show better properties than conventional alloys [5]. AHMCs are the new HMC combination of at least two different types of reinforcements incorporated into an aluminum matrix. Different reinforcements are

added into the aluminum matrix to meet the industrial requirements, such as low cost, good machinability, high strength and hardness, high ductility, good corrosion and wear resistance, and low density. Due to their tempting properties, AHMCs are most frequently used in automobile, aerospace, electrical, and some other engineering industries [6–11].

Aluminum-based hybrid composites have been developed through many processes, such as powder metallurgy (PM), forging, stir casting, spark plasma, and conventional sintering methods [12–17]. Among these processes, the PM method is simple and cost-effective and exhibits better results than the other synthesis processes. The powder metallurgy process is a combination of different steps, including blending, compaction, and sintering. Sintering is an important step that ensures the final hybrid composites' desired physical, microstructural, and mechanical properties. Many methods can conduct the sintering process; however, the microwave sintering (MWS) technique has salient advantages over the conventional sintering process. The MWS process is attractive due to its salient features, including high efficiency, rapid and volumetric heating, uniform heating of the material, and balancing the radiant and microwave heating effects [18–23].

Different types ofreinforcing ceramics used in AHMCs are SiC [24], TiC [25], Al_2O_3 [26], Y_2O_3 [27], TiO_2 [28], ZrO_2 [29], B_4C [30], Si_3N_4 [31], and more. Among these, SiC and TiO_2 are selected as reinforcements in aluminum matrix composites due to their appealing properties. Silicon carbide (SiC) contributes to high hardness, high flexural strength, and good thermal conductivity [32,33]. Similarly, titania (TiO_2) is advantageous because of its high density, high wear resistance, thermal expansion, and electrical resistance [34,35]. The final properties of the hybrid composites are sensitive to the processing parameters, composition, and post-treatment [11,36].

This study was carried out to verify the innovation of the microwave sintering technique and powder metallurgy process in developing Al/SiC/TiO_2 hybrid nanocomposites by examining their viability through material characterization assessments. The focus of this study was directed to the exploration of the effect of TiO_2 nanoparticles' concentrations on the microstructure and mechanical properties of Al/SiC/TiO_2 hybrid nanocomposites. To the best of the authors' knowledge, there has been no report on Al/SiC/TiO_2 hybrid nanocomposites prepared through the microwave sintering process.

2. Experimental Details

2.1. Selection of Raw Materials

Pure Al, SiC, and TiO_2 were used as matrices and reinforcements, respectively, in the development of Al/SiC/TiO_2 hybrid nanocomposites. The specifications of Al, SiC, and TiO_2 nanoparticles are presented in Table 1. The five compositions, fabricated under similar conditions, were A1—pure Al, A2—Al/5SiC, A3—Al/5SiC/3TiO_2, A4—Al/5SiC/6TiO_2, and A5—Al/5SiC/9TiO_2.

Table 1. Specifications of matrix and reinforcement particles.

S. No:	Particles	Purity (%)	Particle Size	Density (g/cc)	Suppliers
1	Al	99.5	7–15 µm	2.70	Alfa Aesar
2	SiC (b-phase)	—	44–55 nm	3.21	Alfa Aesar
3	TiO_2 (anatase)	99.7	15 nm	4.23	Alfa Aesar

2.2. Preparations of Hybrid Nanocomposite Samples

To synthesize the Al/SiC/TiO_2 hybrid nanocomposites, the stoichiometric amounts of precursor materials were weighed carefully by an analytical balance. The weighed powders were blended through a planetary ball mill PM 200 at a speed of 200 rpm for 2 h. The blended powder of approximately 1 gm was taken and compacted into cylindrical pellets with an applied pressure of 50 MPa for 60 s. The compacted green pallets were then sintered using a microwave sintering furnace (VB ceramic furnace, VBCC/MF/1600 °C/14/15, Chennai, India) at a temperature of 550 °C for 30 min, with a heating rate of approximately 10 °C/min. The sintered samples were further used for different characterizations. The

samples were polished and ultrasonically cleaned in an alcoholic solution. A schematic representation of the Al/SiC/TiO_2 hybrid nanocomposites is shown in Figure 1.

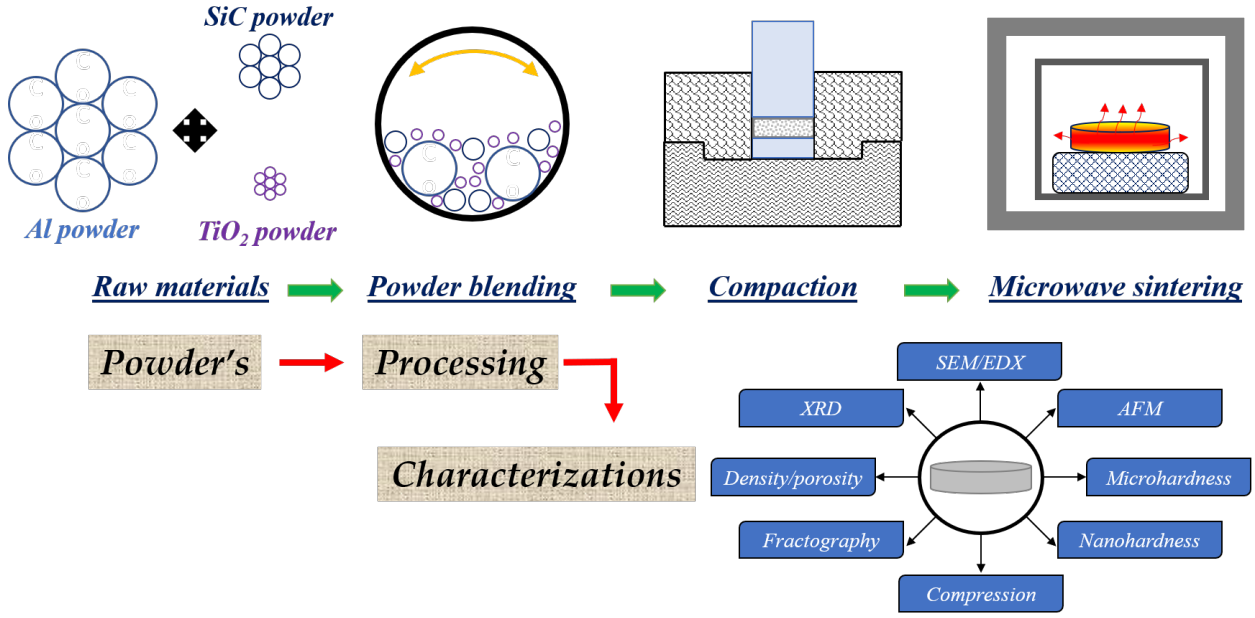

Figure 1. Schematic diagram of the developed Al/SiC/TiO_2 hybrid nanocomposites.

2.3. Characterization

The density and porosity of the Al/SiC/TiO_2 hybrid nanocomposites were measured using Archimedes' principle. XRD analysis was performed on the polished microwave sintered samples using PANalyticalX'pert pro.

The SEM micrographs of the Al/SiC/TiO_2 hybrid nanocomposites were carried out using a field emission scanning electron microscope (SEM-FEI Nova NanoSEM 450 FE-SEM, Hillsboro, OR, USA) with energy-dispersive X-ray spectroscopy (Bruker SDD-EDS, Coventry, UK). The surface roughness of the Al/SiC/TiO_2 hybrid nanocomposites was carried out using an atomic force microscope (MFP-3D Nanoindenter, Columbia, SC, USA).

The Vickers microhardness of the developed Al/SiC/TiO_2 hybrid nanocomposites was measured on a Vickers microhardness tester (MKV-h21) at a load of 50 gf for 10 s. The nanohardness of the hybrid nanocomposites was examined using the MFP-3D Nanoindenter system at a load of 100 mN. For microhardness testing, 4-sided pyramid tips were used, while for nanoindentation, 3-sided pyramid tips were employed. Both micro- and nanohardness experiments were conducted at room temperature (RT), and the reported results are an average of five indentations that were taken for each sample.

The compression strength and yield strength of the developed Al/SiC/TiO_2 hybrid nanocomposites were measured on a universal testing machine (Lloyd-Ametek LR50K Plus) at room temperature under compression loading according to ASTM E9-89a. The average of the 3 samples was taken for each test. The fractured surfaces of the Al/SiC/TiO_2 hybrid nanocomposites were studied using an SEM-FEI Nova NanoSEM 450 FE-SEM scanning electron microscope.

3. Results and Discussion

3.1. Density and Porosity

Figure 2 illustrates the measured density and porosity results of the pure aluminum and its hybrid nanocomposites. It can be seen that the density of the hybrid nanocomposites increased with the increase in the amount of TiO_2. However, the density of the hybrid nanocomposites was higher than that of the base aluminum matrix due to the presence of higher density reinforcements SiC (3.21 g/cc) and TiO_2 (4.23 g/cc) in the Al

matrix (2.7 g/cc). The higher density of the microwave sintered samples influenced the structural, hardness, and strength of the hybrid nanocomposites [14]. It can also be noticed from Figure 2 that the porosity increased with an increase in the contents of TiO_2 nanoparticles in the aluminum matrix. This can be ascribed to the effect of agglomeration at high reinforcement content and pore nucleation formation at the particle reinforcement surface [37–39].

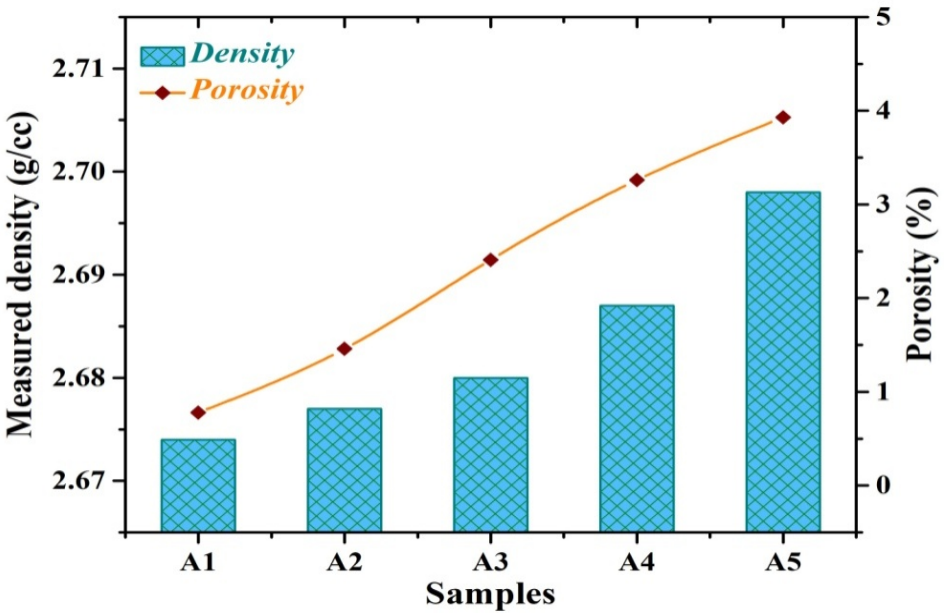

Figure 2. Density and porosity of the Al/SiC/TiO_2 hybrid nanocomposites.

3.2. Phase Identification

Figure 3 shows the XRD (X-ray diffraction) results of the Al/SiC/TiO_2 hybrid nanocomposites. The XRD analysis results confirm the presence of SiC [40] and TiO_2 [41] nanoparticles in the Al matrix [42]. The sharp diffraction peaks of Al were at the 2θangles of 38.6° (111), 44.8° (200), 65.2° (220), and 78.3° (311), very weak peaks of SiC were at the 2θangles of 35.7° (111) and 60.2° (220), and TiO_2 peaks were at the 2θangles of 25.3° (101), 48.2° (004), 54.2° (200), and 55.2° (211). The XRD results confirm that there were no other peaks or impurities present. The presence of a small portion of reinforcements was hard to detect in the XRD spectra. However, the intensity of these peaks increased with an increasing number of reinforcements.

3.3. Microstructure Behavior

The SEM-EDS analysis was performed on the pure Al and its hybrid nanocomposites. Figure 4 shows the SEM micrographs of the pure Al and Al/SiC/TiO_2 hybrid nanocomposites. The SEM micrographs of the specimens clearly show that the SiC and TiO_2 reinforcements were uniformly distributed throughout the aluminum matrix. The light grey surface can beobserved, representing the aluminum matrix, while the dark grey and white spots confirm the presence of SiC and TiO_2 particles, respectively. The selection of suitable ball milling parameters, such as milling speed, time, powder to weight ratio, and so forth, and appropriate microwave sintering parameters, such as sintering temperature, time, power, holding time, and so forth, contributed to producing the compacts with uniform distribution reinforcements. Usually, an increasing percentage in reinforcement leads to an increase in the porosity of the composites, as reflected in Figure 2 [43,44].

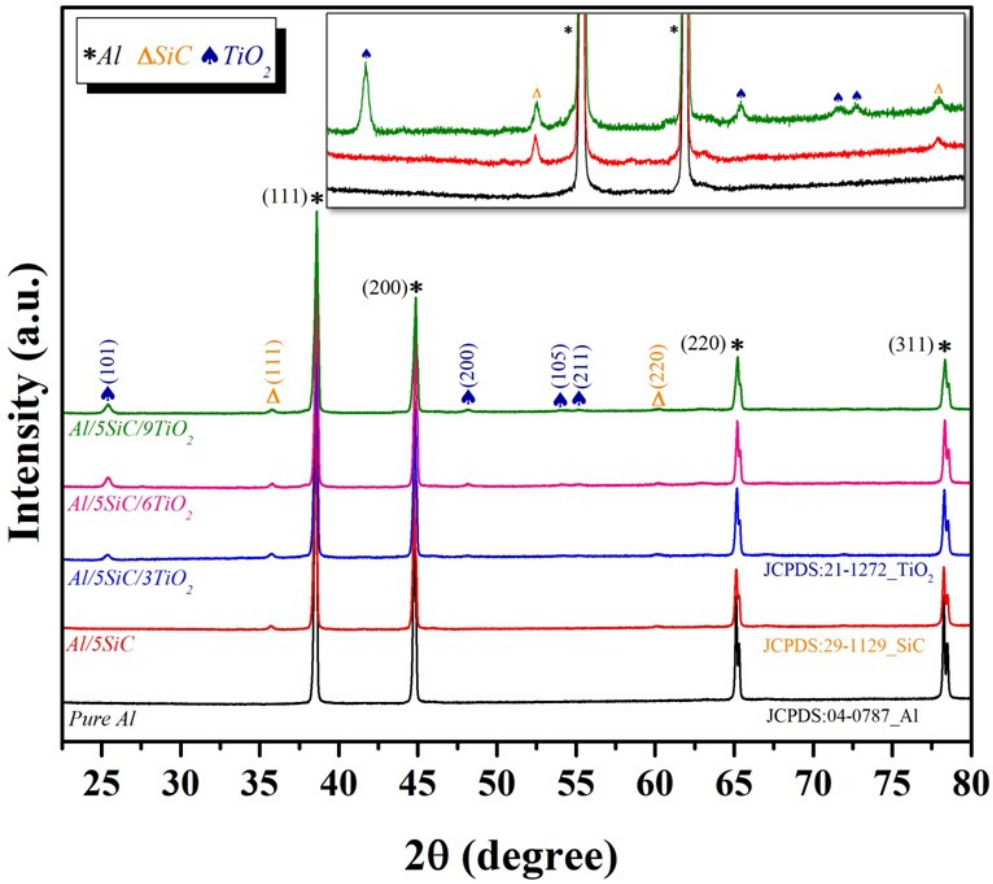

Figure 3. XRD pattern of the Al/SiC/TiO_2 hybrid nanocomposites (inset: magnification image of the pure Al, Al-5SiC, and Al-5SiC-9TiO_2 scale from 20° to 62°).

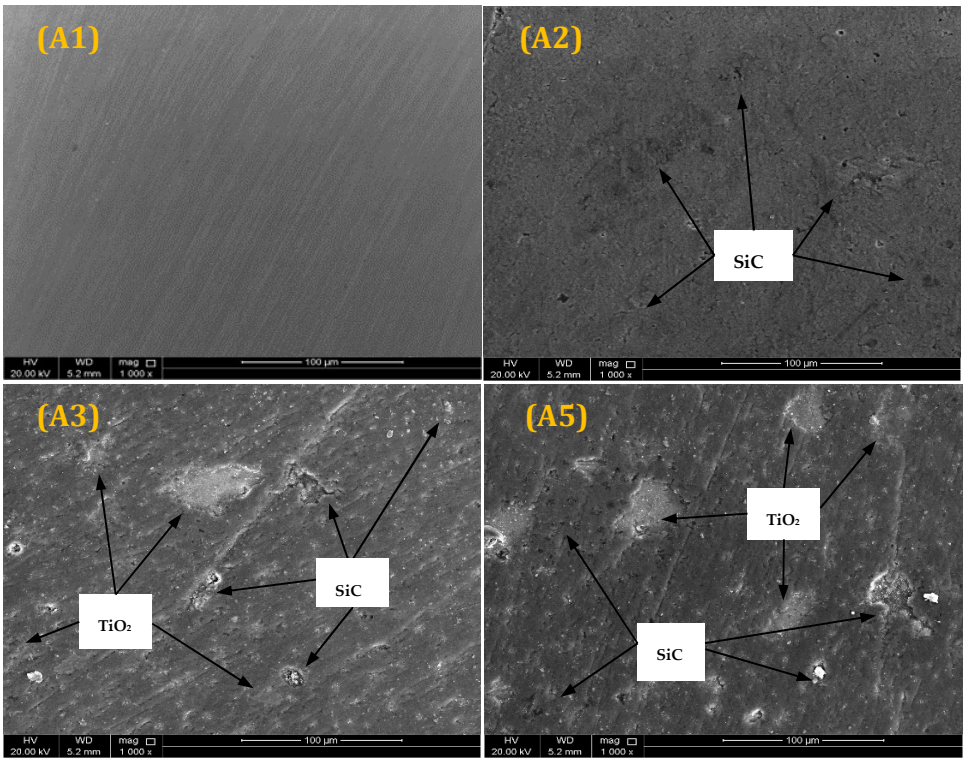

Figure 4. SEM micrographs of the (**A1**) pure Al, (**A2**) Al/5SiC, (**A3**) Al/5SiC/3TiO_2, and (**A5**) Al/5SiC/9TiO_2 hybrid nanocomposites.

The EDS (energy-dispersive X-ray spectroscopy) analysis of the Al/SiC/TiO_2 hybrid nanocomposites is depicted in Figure 5. The EDS spectrum in Figure 5A3–A5 confirms the presence of Al, Si, C, Ti, and O within the Al/SiC/TiO_2 hybrid nanocomposites. Furthermore, Figure 5A5 presents the elemental mapping, which shows that Si (purple), C (blue), Ti (red), and O (yellow) elements were uniformly distributed throughout the Al matrix (green). Consequently, the uniform distribution of Si, C, Ti, and O elements within the Al matrix was successfully achieved.

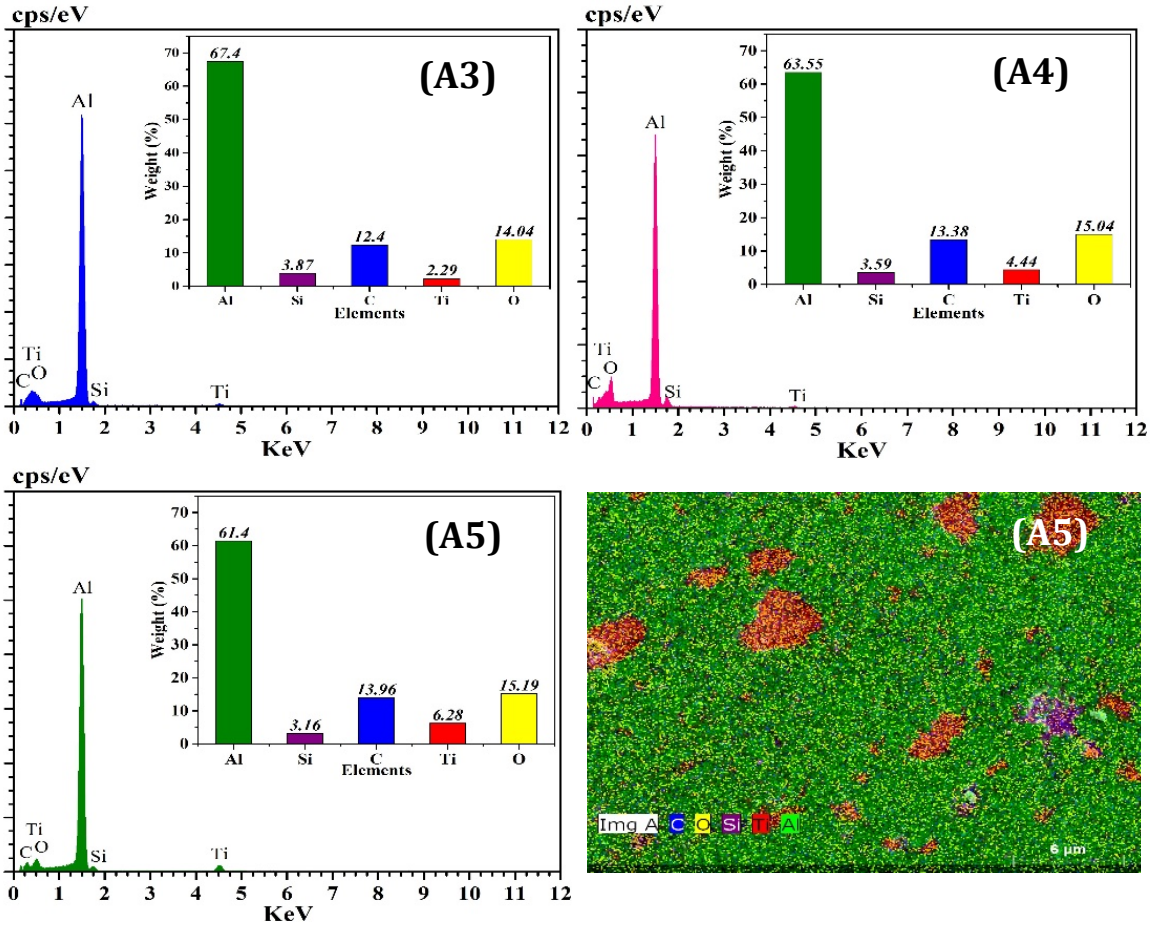

Figure 5. EDX spectra images of (**A3**) Al/5SiC/3TiO_2, (**A4**) Al/5SiC/6TiO_2, and (**A5**) EDX spectra, and elemental mapping of Al/5SiC/9TiO_2 hybrid nanocomposites.

3.4. Surface Roughness

Figure 6 shows the 2D and 3D AFM images of the Al/SiC/TiO_2 hybrid nanocomposites, together with an average surface roughness value. From the AFM analysis, the average surface roughness (R_a) of pure aluminum was 21.793 nm. The average roughness (R_a) of the hybrid nanocomposites increased from 21.793 nm to 34.640 nm with an increase in TiO_2. The average roughness (R_a) of the hybrid nanocomposites is shown in Figure 7. The increase in average roughness (R_a)of Al/SiC/TiO_2 hybrid nanocomposites can be regarded as the effect of insoluble and hard ceramic particles and is consistent with the already reported studies [45,46]. The Al/SiC/TiO_2 hybrid nanocomposites show the varying number of protrusions (hills) and valleys along with the topographic surface, providing an idea about the surface morphology.

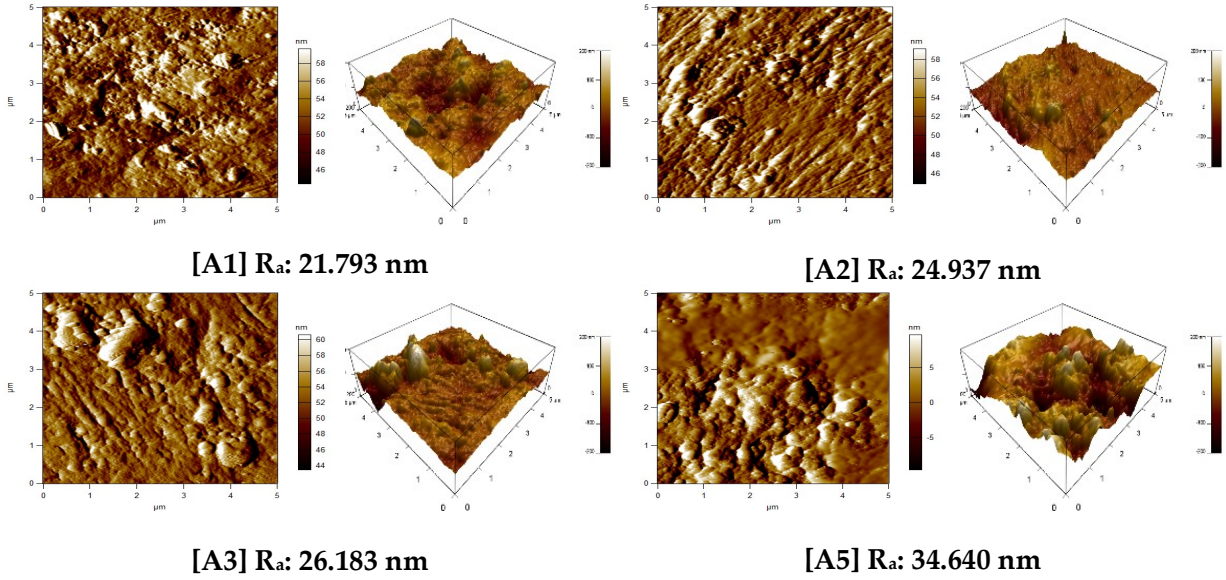

Figure 6. 2D and 3D surface images of (**A1**) pure Al, (**A2**) Al/5SiC, (**A3**) Al/5SiC/3TiO_2, and (**A5**) Al/5SiC/9TiO_2 hybrid nanocomposites.

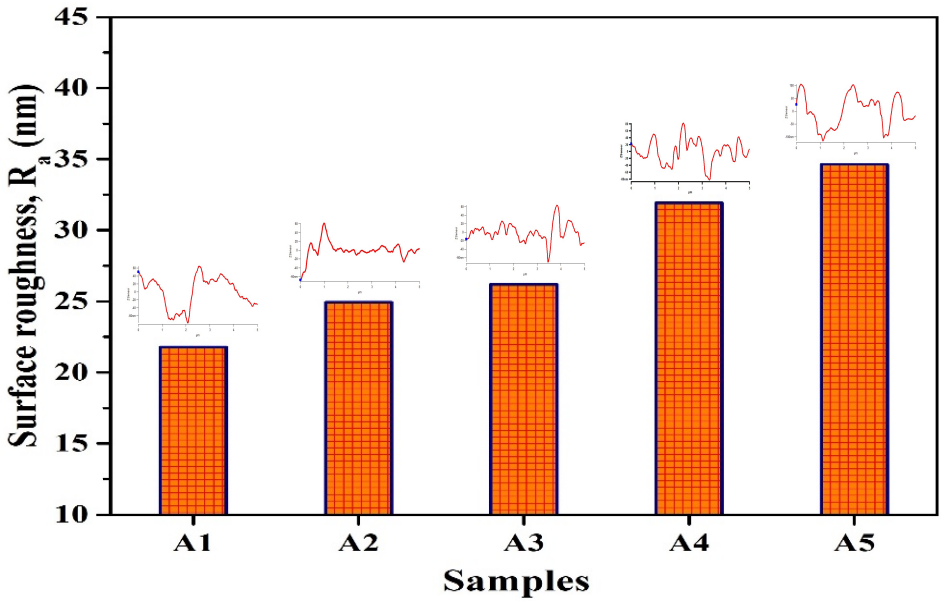

Figure 7. Surface roughness (Ra) data for AFM images of the developed Al/SiC/TiO_2 hybrid nanocomposites with their X profiles.

3.5. Vickers Microhardness

Figure 8 shows the Vickers microhardness results and micrographs of the microhardness indentation of the Al/SiC/TiO_2 hybrid nanocomposites. The corresponding data are summarized in Table 2. The microhardness results show that the Al/SiC/TiO_2 hybrid nanocomposites exhibited higher hardness results than the pure aluminum. Moreover, the hardness of the Al/SiC/TiO_2 hybrid nanocomposites increased with the increasing amount of TiO_2 nanoparticles into the aluminum matrix [47]. The maximum hardness (83 $\pm$ 3 HV) of the hybrid nanocomposites was achieved at 9 wt.% of TiO_2. The improvement in the hardness of the Al/SiC/TiO_2 hybrid nanocomposites can be attributed to the load transfer mechanism. The presence of the hard reinforcements (SiC and TiO_2) in the aluminum matrix offers more resistance to plastic deformation, leading to increased strength and

hardness of the hybrid nanocomposite and an increase in the load-bearing capacity of the hybrid nanocomposites [48].

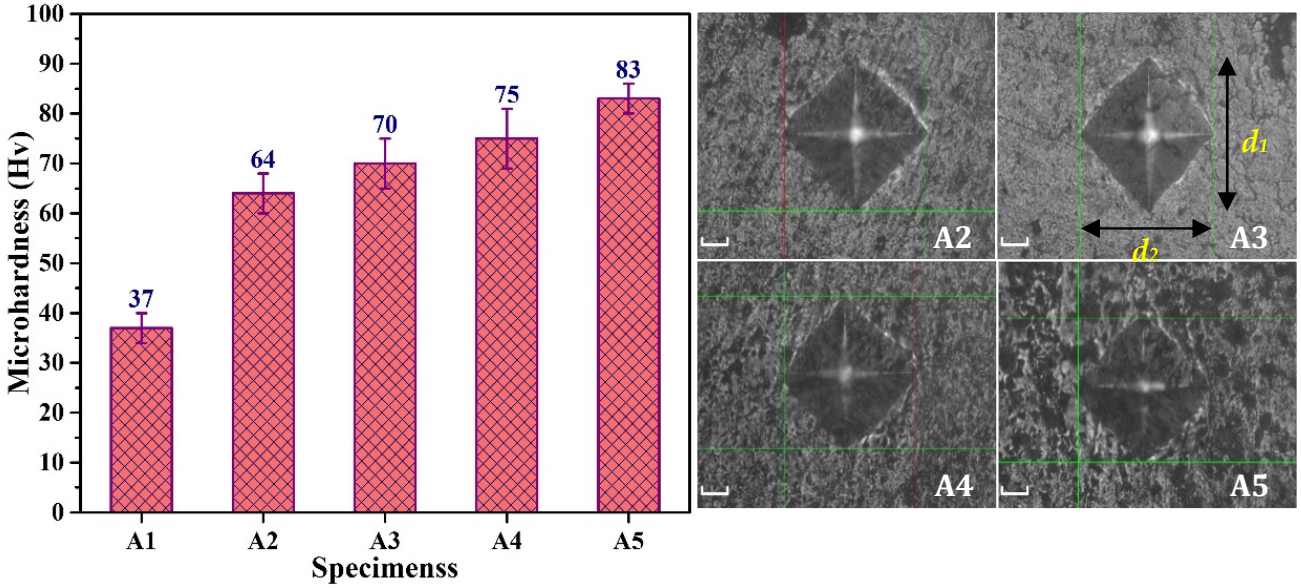

Figure 8. Vickers microhardness of the Al/SiC/TiO_2 hybrid nanocomposites and micrographs of the area indenter by the Vickers hardness tester in samples A2, A3, A4, and A5.

Table 2. Hardnesses and compressive properties of Al/SiC/TiO_2 hybrid nanocomposites.

Specimens	Compositions	Microhardness (Hv)	Nanoindentation (GPa)	UCS (MPa)	CYS (MPa)	Failure Strain (%)
A1	Al	37 ± 3	3.91 ± 0.3	305 ± 6	73 ± 5	>63
A2	Al/5SiC	64 ± 4	4.83 ± 0.2	330 ± 3	89 ± 6	>63
A3	Al/5SiC/3TiO_2	70 ± 5	5.54 ± 0.4	346 ± 5	117 ± 5	>63
A4	Al/5SiC/6TiO_2	75 ± 6	6.12 ± 0.5	359 ± 4	126 ± 6	>63
A5	Al/5SiC/9TiO_2	83 ± 3	7.91 ± 0.7	375 ± 6	139 ± 8	>63

The Vickers microhardness can be determined by the following equation [49]:

$$HV = 1.854\ F/d^2 \quad (1)$$

where F is the load in Kgf and d is the athematic mean of d_1 and d_2 diagonals in mm.

$$d = (d_1 + d_2)/2 \quad (2)$$

3.6. Nanohardness

The load-displacement curves and nanohardness results in the microwave sintered Al/SiC/TiO_2 hybrid nanocomposites containing varying amounts of TiO_2 nanoparticles are shown in Figure 9.

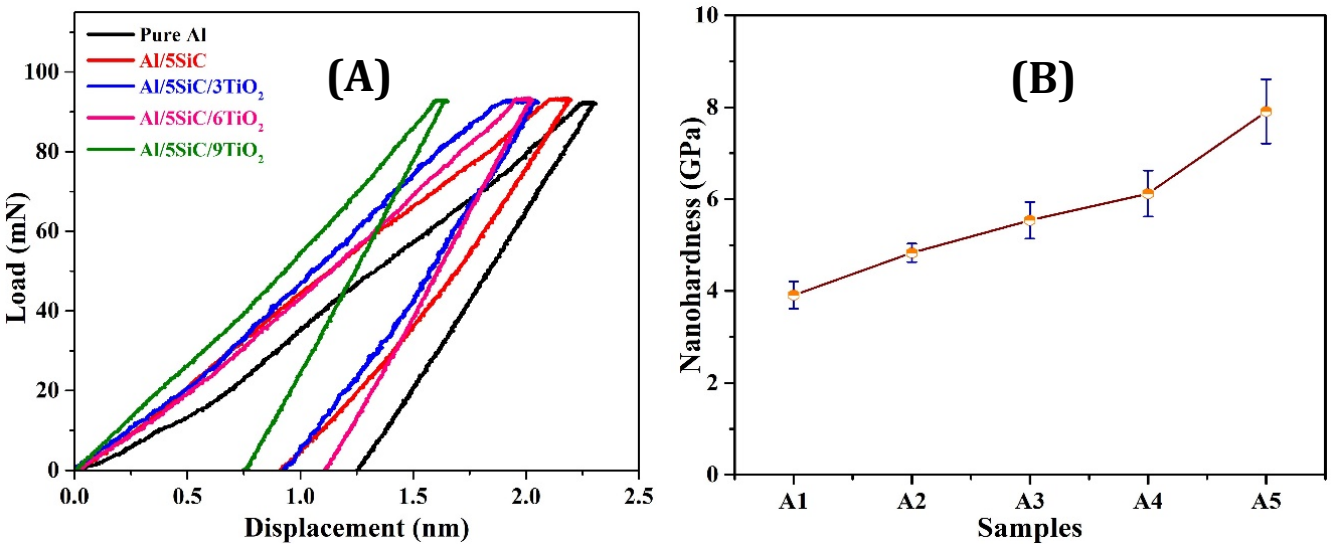

Figure 9. Nanoindentation analysis of Al/SiC/TiO_2 hybrid nanocomposites; (**A**) load/unload-displacement curves and (**B**) nanohardness results.

It can be noticed from the displacement curves in Figure 9A that the penetration depth of the hybrid nanocomposites decreased with the increasing amount of TiO_2 nanoparticles. The decrease in penetration depth indicates the increase in the nanohardness of the hybrid nanocomposites, which agrees with our microhardness results (Figure 8). The lower penetration depth rate is attributed to the higher resistance offered by the aluminum matrix incorporated with hard ceramic nanoparticles. The Al/SiC/TiO_2 hybrid nanocomposites containing 9 wt.% TiO_2 exhibited the best performance, reaching ahardness value of 7.91 GPa.

3.7. Compression and Yield Strength

Figure 10 shows the compressive stress/strain curves and results (yield and compression strength) of the microwave-sintered pure Al and Al/SiC/TiO_2 hybrid nanocomposites. For a clear comparison, the corresponding mechanical data is also shownin Table 2. It can be noticed that Al/SiC/TiO_2 hybrid nanocomposites demonstrated higher strength when compared to the aluminum matrix. Furthermore, the strength of the Al/SiC/TiO_2 hybrid nanocomposites increased with the increasing amount of TiO_2 nanoparticles in the aluminum matrix. The Al/SiC/TiO_2 hybrid nanocomposite containing a 9 wt.% of TiO_2 nanoparticles showed a significant improvement in compressive strength (UCS_375 $\pm$ 6 MPa) and a 0.2% offset compressive yield strength (CYS_139 $\pm$ 8 MPa) as compared to the aluminum matrix.

The improvements in strength and hardness of the hybrid nanocomposites can be attributed to many strengthening mechanisms, as reported in the literature [50–53]. In this present study, the improvements in strength and hardness of the Al/SiC/TiO_2 hybrid nanocomposites were mainly due to the load transfer mechanism, dispersion hardening effect, and Orowan strengthening mechanisms [54,55]. The load transfer mechanism is the most accepted strengthening mechanism that takes place due to the transfer of load (Equation (3)) from weaker matrix material to the harder reinforcements through their interface [56].

$$\Delta\sigma_{load} = 0.5\, f\sigma_m \quad (3)$$

where f is the volume fraction of reinforcements and σ_m is the YS of the matrix (MPa).

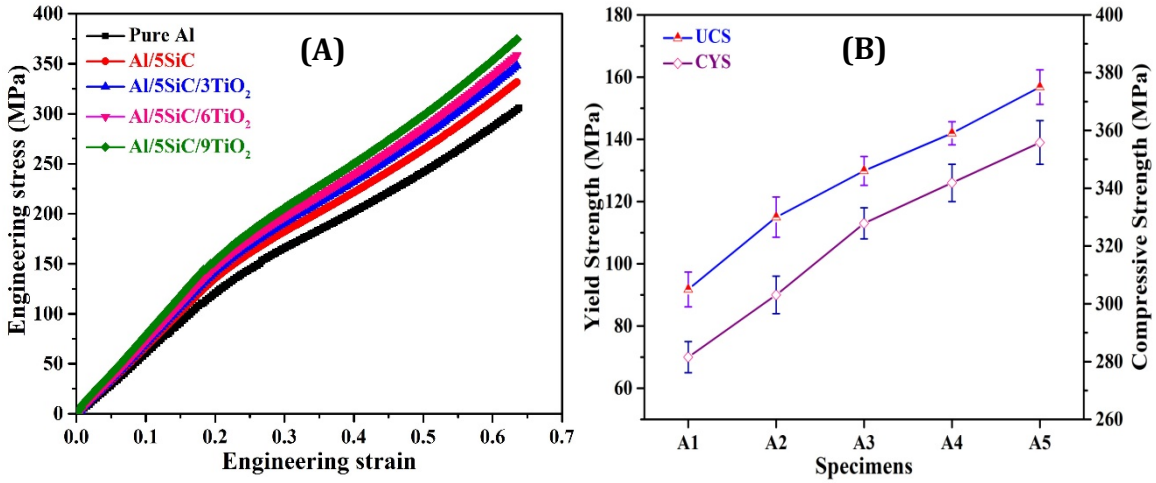

Figure 10. (**A**) Compressive stress/strain curves, (**B**) compressive strength of the Al/SiC/TiO_2 hybrid nanocomposites.

3.8. Fractography

Figure 11 shows the fractography images of the pure aluminum and its hybrid nanocomposites fractured under compression loadings at room temperature. A close comparison suggests a shear mode fracture in the Al/SiC/TiO_2 hybrid nanocomposites. The compressive deformations obtained in the base matrix and hybrid nanocomposites weredifferent due to the dispersion hardening effect. The aluminum matrix's shear fracture was less than the hybrid nanocomposites because the reinforcements in the aluminum matrix acted as secondary phases that restricted the plastic deformation in the aluminum matrix.

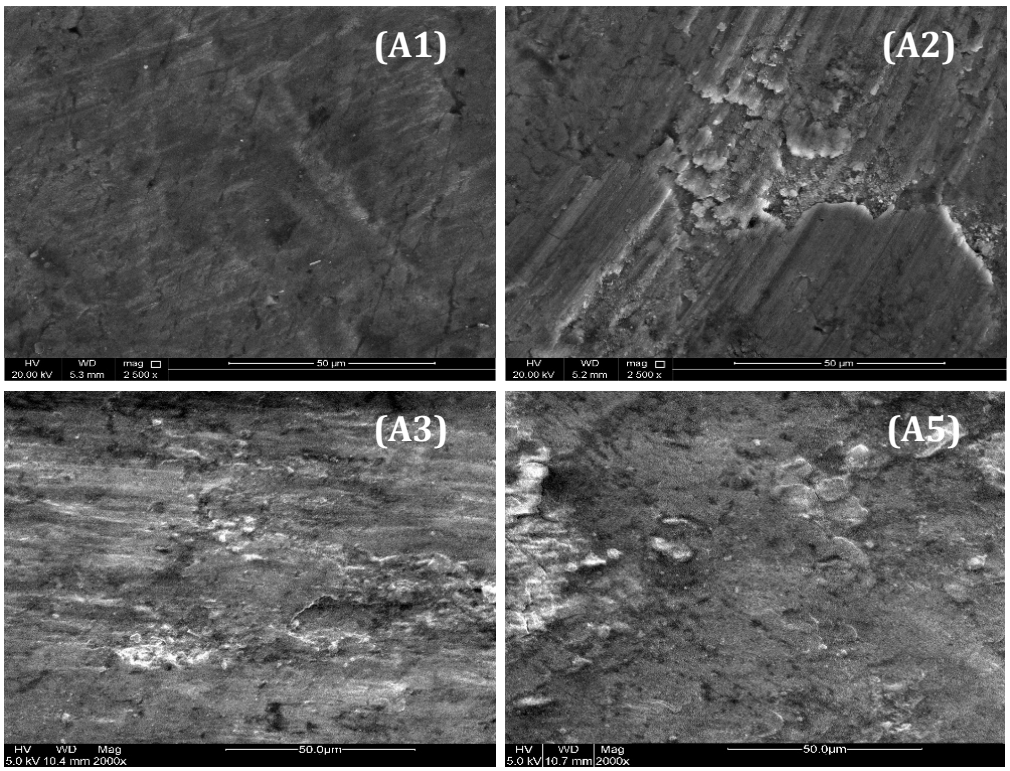

Figure 11. Fracture surface images of the (**A1**) pure Al, (**A2**) Al/5SiC, (**A3**) Al/5SiC/3TiO_2, and (**A5**) Al/5SiC/9TiO_2 hybrid nanocomposites.

4. Conclusions

Al/SiC/TiO_2 hybrid nanocomposites have been successfully synthesized using a combination of powder metallurgy (blending and compaction) and microwave sintering (MWS) techniques. The effects of the concentration of TiO_2 nanoparticles on microstructural and mechanical properties of the developed Al/SiC/TiO_2 hybrid nanocomposites wereinvestigated. The SEM results indicate a uniform distribution of SiC and TiO_2 reinforcements in the aluminum matrix. The nanohardness of the nanocomposites increased from 3.91 $\pm$ 0.3 GPa for pure Al to 7.91 $\pm$ 0.7 GPa for the Al/5SiC/9TiO_2 nanocomposite. Al/SiC/TiO_2 nanocomposites containing 9 wt.% of TiO_2 nanoparticles demonstrated superior hardness (83 $\pm$ 3 Hv), yield strength (139 $\pm$ 8 MPa), and compressive strength (375 $\pm$ 6 MPa) when compared to pure Al. Finally, the Al/SiC/TiO_2 hybrid nanocomposites underwent a shear mode of fracture during their plastic deformation instead of a brittle fracture mode.

Author Contributions: M.R.M. wrote the main part of the manuscript and developed the planning of the experiment. R.H.A., M.Y. and A.A.A. performed characterization of the microstructure and mechanical studies of the samples. A.K. and M.R.M. carried out the preparation of different composite materials and tested physical properties. P.R.M., R.G.K. and R.A.S. supervised the materials preparation process and modified the manuscript draft. All authors have read and agreed to the published version of the manuscript.

Funding: This research received no external funding.

Acknowledgments: Penchal Reddy Matli is thankful to the CSIR, New Delhi, India, for financial support under CSIR-SRA (Scientist's Pool Scheme-13(9188-A)/2021-Pool).The authors are also grateful to the Central Laboratory Unit (CLU) Qatar University for the SEM/EDX analysis.

Conflicts of Interest: The authors declare no conflict of interest.

References

1. Perov, B.V.; Khoroshilova, I.P. *Hybrid Composite Materials BT—Polymer Matrix Composites*; Shalin, R.E., Ed.; Springer: Dordrecht, The Netherlands, 1995; pp. 269–304, ISBN 978-94-011-0515-6.
2. Yamada, A.; Sasabe, H.; Osada, Y.; Shiroda, Y. Concept of hybrid materials, hybrid materials-concept and case studies. *ASM Int.* **1989**, *18*.
3. Chavhan, G.R.; Wankhade, L.N. Improvement of the mechanical properties of hybrid composites prepared by fibers, fiber-metals, and nano-filler particles—A review. *Mater. Today Proc.* **2019**, *27*, 72–82. [CrossRef]
4. Vieira, C.A.B.; Susin, S.B.; Freire, E.; Amico, S.C.; Zattera, A.J. Characterization of hybrid composites produced with mats made using different methods. *Mater. Res.* **2009**, *12*, 433–436. [CrossRef]
5. Pitchayyapillai, G.; Seenikannan, P.; Raja, K.R.; Chandrasekaran, K. Al6061 Hybrid Metal Matrix Composite Reinforced with Alumina and Molybdenum Disulphide. *Adv. Mater. Sci. Eng.* **2016**, *2016*, 1–9. [CrossRef]
6. Bodunrin, M.O.; Alaneme, K.K.; Chown, L.H. Aluminium matrix hybrid composites: A review of reinforcement philosophies; Mechanical, corrosion and tribological characteristics. *J. Mater. Res. Technol.* **2015**, *4*, 434–445. [CrossRef]
7. Ahamed, H.; Senthilkumar, V. Hybrid Aluminium Metal Matrix Composites and Reinforcement Materials: A Review. *Int. J. Innov. Res. Sci. Eng. Technol.* **2016**, *5*, 6284–6288.
8. Rino, J.J.; Chandramohan, D.; Sucitharan, K.S. An Overview on Development of Aluminium Metal Matrix Composites with Hybrid Reinforcement. *IJSR India Online ISSN* **2012**, *1*, 2319–7064.
9. Bhatia, R.S. An Experimental Analysis of Aluminium Metal Matrix Composite using Al_2O_3/B4C/Gr Particles. *Int. J. Adv. Res. Comput. Sci.* **2017**, *8*, 83–90. [CrossRef]
10. Mavhungu, S.T.; Akinlabi, E.T.; Onitiri, M.A.; Varachia, F.M. Aluminum Matrix Composites for Industrial Use: Advances and Trends. *Procedia Manuf.* **2017**, *7*, 178–182. [CrossRef]
11. Singh, J.; Chauhan, A. Characterization of hybrid aluminum matrix composites for advanced applications—A review. *J. Mater. Res. Technol.* **2016**, *5*, 159–169. [CrossRef]
12. Kanthavel, K.; Sumesh, K.R.; Saravanakumar, P. Study of tribological properties on Al/Al_2O_3/MoS_2 hybrid composite processed by powder metallurgy. *Alex. Eng. J.* **2016**, *55*, 13–17. [CrossRef]
13. Murthy, K.V.S.; Girish, D.P.; Varol, T.; Koppad, G.P. Mechanical and thermal properties of AA7075/TiO_2 /Fly ash hybrid composites obtained by hot forging. *Prog. Nat. Sci.* **2017**, *27*, 474–481. [CrossRef]
14. Sambathkumar, M.; Navaneethakrishnan, P.; Ponappa, K.; Sasikumar, K.S.K. Mechanical and Corrosion Behavior of Al7075 (Hybrid) Metal Matrix Composites by Two Step Stir Casting Process. *Lat. Am. J. Solids Struct.* **2016**, *14*, 243–255. [CrossRef]

15. Matli, P.R.; Fareeha, U.; Shakoor, R.A.; Mohamed, A.M.A. A comparative study of structural and mechanical properties of Al-Cu composites prepared by vacuum and microwave sintering techniques. *J. Mater. Res. Technol.* **2018**, *7*, 165–172. [CrossRef]
16. Ghasali, E.; Pakseresht, A.; Rahbari, A.; Eslami-shahed, H.; Alizadeh, M.; Ebadzadeh, T. Mechanical properties and microstructure characterization of spark plasma and conventional sintering of Al–SiC–TiC composites. *J. Alloys Compd.* **2016**, *666*, 366–371. [CrossRef]
17. Khan, A.; Matli, P.R.; Nawaz, M.; Mattli, M.R. Microstructure and Mechanical Behavior of Hot Extruded Aluminum/Tin-Bismuth Composites Produced by Powder Metallurgy. *Appl. Sci.* **2020**, *10*, 2812. [CrossRef]
18. Oghbaei, M.; Mirzaee, O. Microwave Versus Conventional Sintering: A Review of Fundamentals, Advantages and Applications. *J. Alloys Compd.* **2010**, *494*, 175–189. [CrossRef]
19. Chandrasekaran, S.; Ramanathan, S.; Basak, T. Microwave material processing—A review. *AIChE J.* **2012**, *58*, 330–363. [CrossRef]
20. Matli, P.; Shakoor, R.; Amer Mohamed, A.; Gupta, M. Microwave Rapid Sintering of Al-Metal Matrix Composites: A Review on the Effect of Reinforcements, Microstructure and Mechanical Properties. *Metals* **2016**, *6*, 143. [CrossRef]
21. Fliflet, A.W.; Bruce, R.W.; Kinkead, A.K.; Fischer, R.P.; Lewis, D.; Rayne, R.; Bender, B.; Kurihara, L.K.; Chow, G.-M.; Schoen, P.E. Application of microwave heating to ceramic processing: Design and initial operation of a 2.45-GHz single-mode furnace. *IEEE Trans. Plasma Sci.* **1996**, *24*, 1041–1049. [CrossRef]
22. Agarwal, D. Microwave sintering of ceramics, composites and metallic materials, and melting of glasses. *Trans. Ind. Ceram. Soc.* **2006**, *65*, 129–144. [CrossRef]
23. Matli, P.R.; Manakari, V.; Parande, G.; Mattli, M.R.; Shakoor, R.A.; Gupta, M. Improving Mechanical, Thermal and Damping Properties of NiTi (Nitinol) Reinforced Aluminum Nanocomposites. *J. Compos. Sci.* **2020**, *4*, 19. [CrossRef]
24. Reddy, M.P.; Shakoor, R.A.; Parande, G.; Manakari, V.; Ubaid, F.; Mohamed, A.M.A.; Gupta, M. Enhanced performance of nano-sized SiC reinforced Al metal matrix nanocomposites synthesized through microwave sintering and hot extrusion techniques. *Prog. Nat. Sci. Mater. Int.* **2017**, *27*, 606–614. [CrossRef]
25. Karantzalis, A.E.; Wyatt, S.; Kennedy, A.R. The mechanical properties of Al-TiC metal matrix composites fabricated by a flux-casting technique. *Mater. Sci. Eng. A* **1997**, *237*, 200–206. [CrossRef]
26. Hossein-Zadeh, M.; Razavi, M.; Mirzaee, O.; Ghaderi, R. Characterization of properties of Al–Al_2O_3 nano-composite synthesized via milling and subsequent casting. *J. King Saud Univ. Eng. Sci.* **2013**, *25*, 75–80. [CrossRef]
27. Mattli, M.R.; Shakoor, A.; Matli, P.R.; Mohamed, A.M.A. Microstructure and compressive behavior of Al–Y_2O_3 nanocomposites prepared by microwave-assisted mechanical alloying. *Metals* **2019**, *9*, 414. [CrossRef]
28. Ravichandran, M.; Meignanamoorthy, M.; Dineshkumar, S. Microstructure and Properties of Hot Extruded Al-TiO_2 Powder Metallurgic Composites. *Appl. Mech. Mater.* **2016**, *852*, 130–135. [CrossRef]
29. Parveen, A.; Chauhan, N.; Suhaib, M. Mechanical and Tribological Behaviour of Al-ZrO_2 Composites: A Review. In *Lecture Notes in Mechanical Engineering*; Springer: Singapore, 2019; pp. 217–229.
30. Moradi, M.R.; Moloodi, A.; Habibolahzadeh, A. Fabrication of Nano-composite Al-B 4 C Foam via Powder Metallurgy-Space Holder Technique. *Procedia Mater. Sci.* **2015**, *11*, 553–559. [CrossRef]
31. Mattli, M.; Matli, P.; Shakoor, A.; Amer Mohamed, A. Structural and Mechanical Properties of Amorphous Si3N4 Nanoparticles Reinforced Al Matrix Composites Prepared by Microwave Sintering. *Ceramics* **2019**, *2*, 12. [CrossRef]
32. Järrendahl, K.; Davis, R.F. Chapter 1 Materials Properties and Characterization of SiC. In *Semiconductors and Semimetals*; Soo Park, Y.B.T.-S., Ed.; Elsevier: Amsterdam, The Netherlands, 1998; Volume 52, pp. 1–20, ISBN 0080-8784.
33. Choyke, W.J.; Pensl, G. Physical Properties of SiC. *MRS Bull.* **1997**, *22*, 25–29. [CrossRef]
34. Goodfellow Titanium Dioxide—Titania (TiO_2). Available online: http://www.goodfellow.com/E/Titanium-Dioxide.html (accessed on 5 August 2021).
35. Kusior, A.; Banas, J.; Trenczek-Zajac, A.; Zubrzycka, P.; Micek-Ilnicka, A.; Radecka, M. Structural properties of TiO_2 nanomaterials. *J. Mol. Struct.* **2018**, *1157*, 327–336. [CrossRef]
36. Prabu, S.B.; Karunamoorthy, L.; Kathiresan, S.; Mohan, B. Influence of stirring speed and stirring time on distribution of particles in cast metal matrix composite. *J. Mater. Process. Technol.* **2006**, *171*, 268–273. [CrossRef]
37. Elango, G.; Raghunath, B.K. Tribological behavior of hybrid (LM25Al + SiC+ TiO_2) metal matrix composites. *Procedia Eng.* **2013**, *64*, 671–680. [CrossRef]
38. Nassar, A.E.; Nassar, E.E. Properties of aluminum matrix Nano composites prepared by powder metallurgy processing. *J. King Saud Univ. Eng. Sci.* **2017**, *29*, 295–299. [CrossRef]
39. Reddy, M.P.; Ubaid, F.; Shakoor, R.A.; Parande, G.; Manakari, V.; Mohamed, A.M.A.; Gupta, M. Effect of reinforcement concentration on the properties of hot extruded Al-Al_2O_3 composites synthesized through microwave sintering process. *Mater. Sci. Eng. A* **2017**, *696*, 60–69. [CrossRef]
40. Cheng, H.; Tu, R.; Zhang, S.; Han, M.; Goto, T.; Zhang, L. Preparation of highly oriented β-SiC bulks by halide laser chemical vapor deposition. *J. Eur. Ceram. Soc.* **2017**, *37*, 509–515. [CrossRef]
41. Xing, J.; Li, Y.H.; Jiang, H.B.; Wang, Y.; Yang, H.G. The size and valence state effect of Pt on photocatalytic H2 evolution over platinized TiO_2 photocatalyst. *Int. J. Hydrog. Energy* **2014**, *39*, 1237–1242. [CrossRef]
42. Krishna, M.V.; Xavior, M.A. Experiment and Statistical Analysis of End Milling Parameters for Al/SiC Using Response Surface Methodology. *Int. J. Eng. Technol.* **2015**, *7*, 2274–2285.

43. Suarsana, K.; Astika, I.M.; Sunu, P.W. Properties of thermal conductivity, density and hardness of aluminium matrices with reinforcement of sicw/Al_2O_3 hybrid after sintering process. *IOP Conf. Ser. Mater. Sci. Eng.* **2019**, *539*, 012016. [CrossRef]
44. Mokhtar, N.M.; Lau, W.J.; Ismail, A.F.; Ng, B.C. The physicochemical study of polyvinylidene fluoride-Cloisite15A® composite membranes for membrane distillation application. *RSC Adv.* **2014**, *4*, 63367–63379. [CrossRef]
45. Thiagarajan, R.; Palanikumar, K.; Arumugam, S. Synthesis and characterization of sintered hybrid aluminium matrix composites reinforced with nanocopper oxide particles and microsilicon carbide particles. *Compos. Part. B Eng.* **2014**, *59*, 43–49.
46. Ghanaraja, S.; Dileep Kumar, D.J.; Ravikumar, K.S.; Madhusudan, B.M. Mechanical Properties of Hot Extruded Al (Mg)-MnO_2 Composites. *Appl. Mech. Mater.* **2015**, *813–814*, 84–89. [CrossRef]
47. Mohapatra, S.; Mishra, D.K.; Mishra, G.; Roy, G.S.; Behera, D.; Mantry, S.; Singh, S.K. A study on sintered TiO_2 and TiO_2/SiC composites synthesized through chemical reaction based solution method. *J. Compos. Mater.* **2013**, *47*, 3081–3089. [CrossRef]
48. Zhang, Z.; Chen, D.L. Contribution of Orowan strengthening effect in particulate-reinforced metal matrix nanocomposites. *Mater. Sci. Eng. A* **2008**, *483–484*, 148–152. [CrossRef]
49. Denry, I.L.; Holloway, J.A. Elastic constants, Vickers hardness, and fracture toughness of fluorrichterite-based glass-ceramics. *Dent. Mater.* **2004**, *20*, 213–219. [CrossRef]
50. Gladman, T. Precipitation hardening in metals. *Mater. Sci. Technol.* **1999**, *15*, 30–36. [CrossRef]
51. DeGarmo, E.P.; Black, J.T.; Kohser, A.R. *Materials and Processes in Manufacturing*, 10th ed.; Wiley: Hoboken, NJ, USA, 2008; ISBN 9780470055120.
52. Taya, M. Strengthening Mechanisms of Metal Matrix Composites. *Mater. Trans. JIM* **1991**, *32*, 1–19. [CrossRef]
53. Kim, J.G.; Enikeev, N.A.; Seol, J.B.; Abramova, M.M.; Karavaeva, M.V.; Valiev, R.Z.; Park, C.G.; Kim, H.S. Superior Strength and Multiple Strengthening Mechanisms in Nanocrystalline TWIP Steel. *Sci. Rep.* **2018**, *8*, 1–10. [CrossRef]
54. Callister, W.D.; Rethwisch, D.G. *Fundamentals of Materials Science and Engineering*, 3rd ed.; John Wiley & Sons, Inc.: Hoboken, NJ, USA, 2000; ISBN 9780470125373.
55. Ardell, A.J. Precipitation hardening. *Metall. Trans. A* **1985**, *16*, 2131–2165. [CrossRef]
56. Nardone, V.C.; Prewo, K.M. On the strength of discontinuous silicon carbide reinforced aluminum composites. *Scr. Metall.* **1986**, *20*, 43–48. [CrossRef]